Available online at www.sciencedirect.com
ScienceDirect
C. R. Physique 8 (2007) 374–384
COMPTES RENDUS PHYSIQUE
http://france.elsevier.com/direct/COMREN/

Optical techniques for direct imaging of exoplanets/Techniques optiques pour l'imagerie directe des exoplanètes

Detecting extra-solar planets with the Japanese 3.5 m SPICA space telescope

Lyu Abe [a,*], Keigo Enya [b], Shinichiro Tanaka [c,b], Takao Nakagawa [b], Hirokazu Kataza [b], Motohide Tamura [a], Olivier Guyon [d]

[a] *Optical and Infrared Astronomy Division & Extra-solar Planet Project Office, National Astronomical Observatory of Japan, Osawa 2-21-1, Mitaka-city, 181-8588 Tokyo Prefecture, Japan*

[b] *Department of Infrared Astrophysics, Institute of Space and Astronautical Science, Japan Aerospace Exploration Agency, Yoshinodai 3-1-1, Sagamihara, Kanagawa 229-8510, Japan*

[c] *Department of Physics, Graduate School of Science, University of Tokyo, Hongo 7-3-1, Bunkyo-ku, Tokyo 113-0033, Japan*

[d] *Subaru Telescope, National Astronomical Observatory of Japan, 650 North Aohoku Place, Hilo, HI 96720, USA*

Available online 4 June 2007

Abstract

We present the 3.5 m SPace Infrared telescope for Cosmology and Astrophysics (SPICA) space telescope, the launch of which is schedule around year 2015 by the Japanese HII-A rocket, and specifically discuss its use in the context of direct observation of extra-solar planets. This actively cooled (4.5 K), single aperture telescope will operate in the mid and far infrared spectral regions, and up to submillimetric wavelengths (200 μm). The lowest spectral region (5 to 20 μm), where the spatial resolution is the most favorable, will be dedicated to high contrast imaging with coronagraphy. This article describes the SPICA coronagraph project in terms of science, as well as our efforts to study a suitable instrumental concept, compatible with the constraints of the telescope architecture. ***To cite this article: L. Abe et al., C. R. Physique 8 (2007).***

© 2007 Académie des sciences. Published by Elsevier Masson SAS. All rights reserved.

Résumé

Détecter des planètes extra-solaires avec le télescope spatial japonais de 3.5 m SPICA. Nous présentons le télescope spatial SPICA (*SPace Infrared telescope for Cosmology and Astrophysics*) dont la date de lancement est prévue aux alentours de 2015 grâce au lanceur japonais HII-A. Nous discutons plus spécifiquement de son utilisation pour la detection et l'observation directe des planètes extra-solaires. Ce télescope refroidi à 4,5 K, avec son miroir monolithique de 3,5 m, est principalement conçu pour observer dans l'infra-rouge moyen et lointain, et jusqu'aux longueurs d'ondes submillimétriques (200 μm). En raison de la faible résolution angulaire à ces longueurs d'ondes, la partie basse du spectre (de 5 à 20 μm) sera utilisée pour l'imagerie à très haute dynamique par coronographie. Cet article décrit le projet du coronographe de SPICA du point de vue des objectifs scientifiques, mais également de nos efforts dans l'étude d'un concept coronographique compatible avec les contraintes imposées par l'architecture du télescope. ***Pour citer cet article : L. Abe et al., C. R. Physique 8 (2007).***

© 2007 Académie des sciences. Published by Elsevier Masson SAS. All rights reserved.

Keywords: Exoplanets; Coronagraphy; Spectroscopy; Space telescope

* Corresponding author.
E-mail addresses: abe@optik.mtk.nao.ac.jp (L. Abe), enya@ir.isas.jaxa.jp (K. Enya), stanaka@subaru.naoj.org (S. Tanaka), nakagawa@ir.isas.jaxa.jp (T. Nakagawa), kataza@ir.isas.jaxa.jp (H. Kataza), hide@optik.mtk.nao.ac.jp (M. Tamura), guyon@subaru.naoj.org (O. Guyon).

1631-0705/$ – see front matter © 2007 Académie des sciences. Published by Elsevier Masson SAS. All rights reserved.
doi:10.1016/j.crhy.2007.02.007

Mots-clés : Exoplanètes ; Coronographie ; Spectroscopie ; Télescope spatial

1. Introduction

The solar planetary system including the Earth;
Is such system unique in the Universe, or commonplace?
How is such planetary system born? And finally, how about the origin of the life?

We consider that these are three of the most important questions for space science in the near future, and have been making efforts to tackle ways to answer them. Since the first unambiguous confirmation by Mayor and Queloz of the existence of extra-solar planets (or exoplanets) in 1995 [1], more than 200 extra-solar planets have been discovered, mostly by using the radial velocimetry method. Detection of exoplanets is also possible by the transit method [2]. In this case, high accuracy monitoring of the luminosity of stars is needed. When an exoplanet is aligned to the line of the sight of the central star, the luminosity of the star is reduced by the eclipse produced by the planet, and therefore the presence of the planet is inferred. However, such indirect observations do not usually provide the spectrum (although it does to some extent for transits [3]), luminosity and other important properties of the planet itself. Therefore, a systematic study of extra-solar planets by direct observation is required, where the enormous contrast between the central star and planet is the most serious problem. Typically, for Earth-like planets in our Solar system, the contrast is $\sim 10^{-10}$ in the visible light region but is reduced to $\sim 10^{-6}$ in the mid-infrared. Because of this large contrast, clear direct detection has not yet been achieved, in spite of its scientific importance. Development of coronagraphy for exoplanet searching is still extremely challenging because of requirements in terms of high contrast and angular resolution: for example, the angular separation between the sun and Jupiter seen from 10 parsecs distance is only 0.5 arcsec. In this case, if a typical telescope without coronagraph is used, the direct detection of faint planets is still impossible because of the diffraction halo luminosity of the bright star, which is still much too bright at small angular separation. Up to now, many new different coronagraph concepts have been invented to achieve this halo suppression, but none of them has yet delivered valuable scientific results.

However, some of them have been successfully tested in laboratory experiments, which is also a significant part of our work. In this article, we introduce the SPace Infrared telescope for Cosmology and Astrophysics (SPICA) mission [4,5] (Fig. 1) and our progress developing a coronagraph instrument to realize the direct detection of extra-solar planets [6–8]. It is one of the first Japanese space missions comprising a high-contrast coronagraph to directly detect exoplanets. The primary targets of the SPICA coronagraph are giant/Jovian-type exoplanets. Because of its wavelength coverage (5 to 200 μm) and primary mirror diameter (3.5 m), its angular resolution will be limited to the exploration of outer planets (i.e. beyond 5 AU to their host star). Owing to the direct observation of the Jovian-type

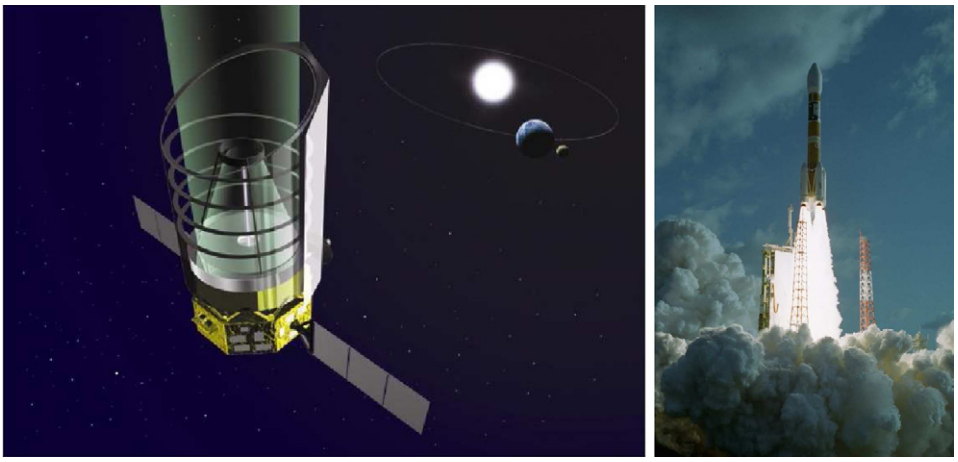

Fig. 1. (Left) artist view showing the SPICA telescope concept, and (right) a HII-A rocket (© by JAXA).

exoplanets by SPICA, we expect to characterize exoplanetary systems and reveal their formation history in advance of the missions targeting terrestrial planets (e.g., TPF [9,10], DARWIN [11], JTPF [12]).

First, we present an overview of the SPICA mission in terms of focal instrumentation and scientific goals, including exoplanet science. Then we consider the specifications of a coronagraph with the constraints of the SPICA telescope opto-mechanical design. We describe several envisaged coronagraphs and our efforts in several laboratory experiments.

2. Extra-solar planet search road-map

There have been some high-contrast imaging activities in Japan. It is useful to summarize them with a road-map. The first one began some years back with the development and use of the CIAO (Coronagraphic Imager with Adaptive Optics [13]) at the 8.2 m Subaru telescope located in Hawaii, and the last milestone of that road-map should be the J-TPF (Japanese Terrestrial Planet Finder) [12], a visible, space telescope dedicated to high-contrast imaging. There several important steps are to be achieved, however, on the way to terrestrial planet detection, taking into account the many scientific studies and results achieved in the extra-solar planets field (including disk and, more generally, star formation science). The first one is the replacement of the CIAO coronagraph on the Subaru telescope, by its second generation equivalent, the HiCIAO [14]. This completely new instrument is expected to provide contrasts up to 10^{-6} near $1.0''$ in the nIR bands (JHKs). However, one important aspect of HiCIAO is that it has been developed with the clear intention to use it as a kind of test-bed for new technologies or concepts. Needless to say, this strategy is accompanied by the emergence of several groups working together in that field on a coherent basis. This includes, of course, the SPICA coronagraph development, which is the next milestone, following the ground-based operation of HiCIAO. The SPICA coronagraph will be the first high-contrast instrument launched in space by Japan and thus constitutes a very important step for the future. The path to the J-TPF is nonetheless also oriented to international collaborations, and can be related to the NASA TPF project in many ways. The overall efforts put into this type of crucial scientific mission will determine whether J-TPF will be a stand-alone Japanese mission, or if it will be a Japanese partnership to a more international project.

3. The SPICA mission

3.1. Overview

The Space Infrared telescope for Cosmology and Astrophysics (SPICA) is the next generation space-borne telescope mission led by Japan Aerospace Exploration Agency (JAXA) following on AKARI, which was developed by the Institute of Space and Astronautical Sciences (ISAS)/JAXA and launched in February 2006 [4]. Because SPICA is a general purpose observatory, the target objects of SPICA are quite widely distributed, e.g., objects in the solar system, planets in and out of the solar system, star formation and evolution, the center of our galaxy, extra galaxies, active galactic nuclei and the infrared cosmic background are important targets. We are developing a mid infrared cononagraph for SPICA as one of the focal plane instruments (Fig. 2, left). In this section, first we introduce the SPICA mission, and then we provide a scientific description focused on coronagraphic observation.

The SPICA telescope will be launched in the middle of 2010s onboard an HII-A Rocket. Fig. 1 shows an artist view of the SPICA telescope in orbit (left) and a HII-A rocket (right). Many efforts were dedicated to the study of the cryogenic system of the telescope to cool it down to 4.5 K, as the telescope will be warm-launched, and cooled-down in situ by the combination of the radiation cooling and mechanical cryo-coolers. This approach using no cryogenic liquid is essentially new: in the case of the Japanese infrared astronomical satellite AKARI (previously named ASTRO-F),[1] a liquid helium tank is combined with a mechanical cooler to cool its 68.5 cm telescope down to 6.5 K. A similar cryogenic system design can be found on the Spitzer Space Telescope with its 85 cm aperture. Elimination of the cryostat and the cryogenic liquid tank is the most important reason why the SPICA telescope can be large [15] (Fig. 3).

[1] AKARI was successfully launched by Japan onboard a Mu-V rocket, on 21 February 2006 from the Uchinoura launch site.

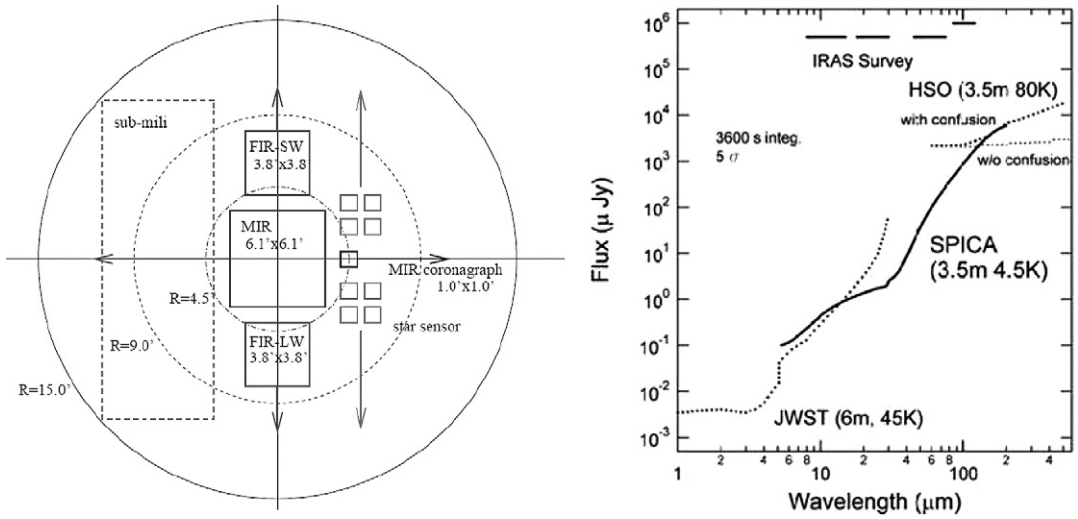

Fig. 2. (Left) distribution of focal plane for the expected instrumentation. (Right) Sensitivity comparison between JWST and SPICA.

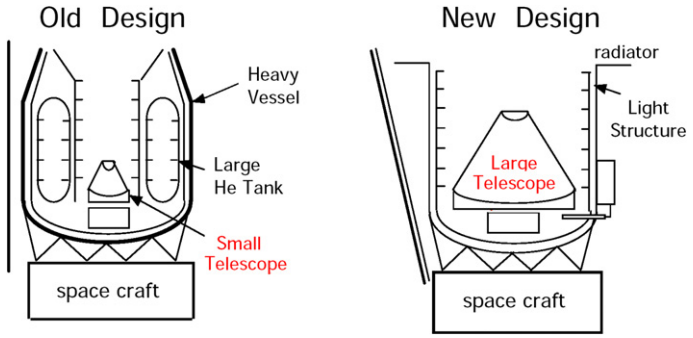

Fig. 3. Concept of the cooling system of previous satellite for infrared astronomy and SPICA.

The baseline concept is an on-axis telescope in a Ritchey–Chretien optical configuration. This design requires a large secondary mirror, which is not highly recommended for most coronagraphs. In the current design, the secondary mirror diameter will be between 15 and 25% of the primary mirror diameter. The structure of the telescope will be made of SiC (silicon carbide) or C/CiC (carbon-fiber reinforced SiC), including the secondary supporting structure in a perpendicular cross-shaped design (and 12 cm in width). The SiC or C/SiC primary mirror will be cooled down to 4.5 K by cryo-coolers using a technology similar to that of the AKARI telescope. This temperature implies a number of constraints on the optics, especially for the coronagraphic part which requires a high quality wavefront prior to entering the coronagraph. Therefore, the primary mirror deformations need to be compensated by an active or adaptive system. Moreover, the cryo-cooler will generate some vibrations producing a large pointing error of about $3''$ which is much too large for the coronagraphic requirements.

The SPICA coronagraph can be compared to the JWST instrumentation which will also include some coronagraphic capabilities (Fig. 2, right). Indeed, although the SPICA telescope will be cooled down to 4.5 K (compared to 70 K for JWST), it will only benefit from an increased sensitivity in the spectral regions above 25 μm. This is mostly due to the difference in size of the two primary optics (6 m versus 3.5 m). However, the SPICA coronagraph has certain merits over the JWST coronagraph. First, the monolithic mirror of the SPICA telescope is more suitable for coronagraphy than the segmented mirror of the JWST. The complex segment geometry requires an equally complex Lyot stop for the suppression of the diffracted light by each segment. Secondly, the SPICA telescope itself being cold (4.5 K), it is optimized for mid-infrared (and far-infrared) astronomy, thus matching the optimization of the instrument. Thirdly, the proposed SPICA coronagraph aims not only for coronagraphic imaging but also for coronagraphic spectroscopy. In order to achieve the spectroscopic capability, we will develop a Ge or CdTe grism with a high efficiency ($>80\%$).

Currently an efficiency of ∼60% is achieved (N. Ebizuka, private communication). The resolving power of the grism is a few hundreds. Long-slits with central occulting block (square in shape) will be available.

3.2. Disks and extra-solar planets science

Many investigations are currently paving the way to the understanding of planetary formation and evolution. Theorists are addressing the complex mechanisms and evolutionary stages of primordial material from the stellar nebula. The exact planetary formation scenarios have not yet been determined; the two competing processes for forming Jupiter-like, gaseous planets include either a rapid gas collapse into denser regions originating from gravitational instabilities in the disk, or a slower formation of solid cores that end up attracting surrounding gas (core accretion model). Understanding the intrinsically complex structures that are expected from these models will necessarily benefit from direct imaging capabilities. The early phases of planetary formation are of particular importance since they will discriminate between the formation processes. At this stage, probing the disks structure is a very important task so that mid infrared observation are crucial in this context.

Spectral energy distributions of exoplanets are composed of the reflecting component dominant at optical and near-infrared wavelengths and the thermal component dominant at mid-and far-infrared wavelengths. For the Sun and Jupiter, the flux contrast is 9 orders of magnitude where the reflection component is dominant and goes down to 6 orders of magnitude where the thermal component becomes dominant at longer wavelengths. Although these can be regarded as a superposition of two blackbody spectra with different temperatures (e.g. about 6000 K for the sun and 140 K for Jupiter), the real spectra of planets are far from that of a blackbody due to the rich features of the planetary atmosphere. These features are very useful for examining and characterizing the exoplanets and cold brown dwarfs. It is noteworthy to remember that our proposed coronagraphic spectrometer has the wavelength coverage and the spectral resolution similar to those of the infrared spectrometer on the Voyager spacecraft (IRIS, Infrared Interferometer Spectrometer and Radiometer). IRIS is a Fourier spectrometer with a wavelength coverage from 4 to 56 μm and a spectral resolution of 40–600. While IRIS played an important role for revealing the atmospheric compositions of the four giant planets of our solar system (Jupiter, Saturn, Uranus, Neptune [16,17]), the coronagraphic spectrometer of SPICA will be an important tool for the study of exoplanets. Notable features expected in the atmospheric spectra of exoplanets, and the corresponding science, are as follows:

1. There is a remarkable peak around 4–5 μm whose flux is significantly larger than the blackbody flux. This peak corresponds to an opacity 'window' for very-low mass and cold objects and is expected to be commonly seen in any objects with temperatures between 100 and 1000 K [18]. Planets with very low temperature, such as the Jupiter, have a peak at 5 μm, while hotter objects tend to have a peak at 4 μm.
2. CNO abundance relative to H can be compared among the exoplanets and the solar system planets. Notable features in the wavelength coverage of the proposed instrument are CH_4 at 7.7 μm, H_2O at 6.3 μm, and NH_3 at 10.7, 10.3, and 6.1 μm.
3. It is well known that the He abundance shows a large variation among giant planets [17]: the helium mass fraction is 0.06 for Saturn, 0.18 for Jupiter, 0.26 for Uranus, 0.32 for Neptune, and 0.28 for the proto-Sun. It would be intriguing to find such a variation among exoplanets. One of the methods to estimate the He/H ratio is the use of the He–H_2 and H_2–H_2 collision-induced absorption band features around 17 μm [19].
4. As a way to make a distinction between brown dwarfs and exoplanets, it will be useful to see the deuterium depletion from the CH_3D feature around 8.6 μm.
5. It will also be interesting to find disequilibrium species such as PH_3 (4.3, 8.9, 10.1 μm) and GeH_4 (4.7 μm) in exoplanets and brown dwarfs.
6. Information on the planet weather or the day/night-side spectra of the planets can be obtained from a monitoring of the time variation of the spectra.

3.3. Observational range for exoplanets

The SPICA coronagraphic instrumentation will be dedicated to the direct detection and characterization of outer extrasolar planets. Considering the luminosity contrast between the host star and the planet, the mid-infrared is a more favorable spectral region for direct observation of extrasolar planets at the expense of angular resolution. Due its ef-

fective temperature of about 120 K, the contrast of a Jupiter-like planet around a Solar-type star becomes smaller than 10^{-6} beyond 16 μm, but dramatically increases up to 10^{-9} below that wavelength, where the only contribution to the observable signal is the starlight reflection on the planet surface. Therefore, at the shortest considered wavelength (5 μm), Jupiter-like planets (around 5 AU) are still extremely challenging, so that hotter planets need to be considered. At longer wavelengths, where the star-to-planet contrast should be smaller, we will be limited by the angular resolution. For stars within 10 pc, the exploration field will therefore be set by the spectral range, and by the coronagraph potential in terms of Inner and Outer Working Angles (IWA and OWA, i.e. the smallest distance where a planet can be detected unambiguously). With a 10 pc distance, at the lowest wavelength (5 μm), the diffraction limit corresponds to a planet distance of 3 AU. Considering that the coronagraph IWA is at best $1.5\lambda/D$, the smallest possible IWA will be around 5 AU. Under the current specifications for the telescope optics, the OWA will probably be limited by the DM specification and/or by the coronagraph type to be used (see below). At present, the baseline OWA is set to around $10\lambda/D$, which corresponds to 30 AU for a 10 pc distance at 5 μm and more than 100 AU at 20 μm (but the IWA will also increase to 12 AU in the best cases). Provided a contrast of 10^{-6} can be reached within this exploration field, the possible targets are self luminous planets of ages between 1–2 Gy and around a few Jupiter masses.

4. The SPICA coronagraph

4.1. Requirements and constraints

The primary goal of our laboratory experiments is to validate the expected performance of several new coronagraphic concepts that could potentially achieve the required contrast and fulfill the requirements. The second point is to clearly identify a baseline coronagraphic solution that would be a compromise between implementation complexity and performance. Due to the poor angular resolution at mIR wavelengths for a 3.5 m telescope diameter, the IWA was clearly identified as a critical issue for the coronagraph. However, a smaller IWA, close to the theoretical limit of $\sim 1.5\lambda/D$ distance, also means higher sensitivity to pointing errors. In the case of the SPICA telescope, the pointing accuracy is rather poor. To solve for this difficulty, a cryogenic tip-tilt mirror has been developed independently from the coronagraph. This mirror offers a correction of 30 milli-arcsec RMS, which corresponds to $\lambda/10$ RMS at $\lambda = 5$ μm, but we find this value is still too large for a number of very high contrast coronagraphs. Some other concepts can manage moderate tip-tilt errors (like the PIAA [20]), and some are almost completely insensitive to tip-tilt jitter; there are, mainly, pupil apodizer concepts with shaped apertures [21]. We are currently precisely studying the possibility of implementing these two types of coronagraphs. Both concepts are described in Section 4.3.

4.2. Adaptive optics

The primary scientific objectives of SPICA were unrelated to coronagraphy, so the telescope was not designed with high-contrast science in mind. The baseline surface roughness specifies a 0.35 μm RMS value, that is, about $\lambda/15$ at 5 μm. With this optical quality, using a coronagraph alone is almost useless, since the requirement to reach a very high contrast coronagraphic image is on the order of $\lambda/1000$ RMS. Therefore, a deformable mirror with a significant number of actuators ($N \times N$ actuators can in principle 'clean' the focal plane diffraction halo up to $N/2\lambda/D$) is mandatory. Several studies [22] have shown that an adaptive mirror coupled to a classical pupil plane wavefront sensor (e.g. Hartmann–Shack), that is, classical adaptive optics, is not adequate for use with a high contrast coronagraph. This is mostly due to the high-frequency components of the wavefront errors being 'folded-back' to low frequencies. It is possible, however, to use alternative wavefront compensation, using so-called *speckle control* or *speckle nulling* techniques.

4.3. Results from laboratory experiments

Binary shaped pupil [23] masks were invented and largely tested in the 1960s as ways to strongly attenuate the diffraction halo in optical systems by diffracting the light along preferential directions. More recently, binary shaped pupils of various kinds appeared [21], some of them recalling binary versions of linear apodizers which are commonly used in laser experiments in order to convert Gaussian beams into flat beams (so called *beam shaping* techniques). Binary shaped pupil masks offer the advantage of being achromatic, meaning that the effect is in principle similar

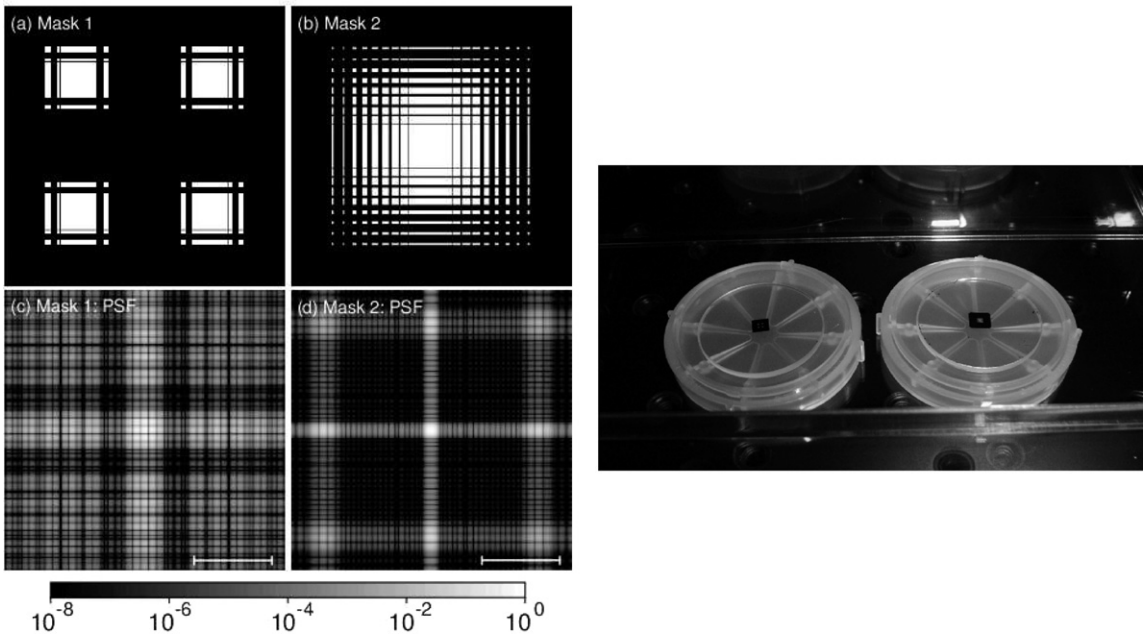

Fig. 4. Left: Panels (a) and (b) show the Mask 1 and Mask 2 designs. The transmission through the black and white regions is 0 and 1, respectively. The diameter of the circumscribed circle to the transmissive part is 2 mm. Panels (c) and (d) show the expected (theoretical) PSFs for Masks 1 and 2. The respective diagonal profiles are shown in Fig. 5. The scale bar is $20\lambda/D$. Right: photographs showing the fabricated Mask 1 (left) and Mask 2 (right) on BK7 substrates. The diameter and thickness of the substrates is 30.0 mm and 2.0 mm, respectively. The translucent cases beneath the substrates are used to transport the devices.

regardless of the wavelength. For the SPICA coronagraph, the checkerboard mask offers a solution compatible with both central obstruction and supporting spider arms. The other advantage of pupil masks is that they have minimal sensitivity to tip-tilt errors/pointing errors. Indeed, in this case, and contrary to other 'focal plane' coronagraphs for example, the coronagraphic PSF is invariant by translation, meaning that the observed coronagraphic image is the convolution product between the object intensity distribution and the unique coronagraphic impulse response (i.e. across all the field).

In the context of SPICA, this kind of binary mask has the huge advantage of having a very simple implementation. The optical setup can be reduced to a minimal configuration where focusing optics are simply located after the binary mask. However, the drawback is that the achievable IWA is very high compared to other coronagraphs. In particular, the size of the central obstruction is the IWA limiting factor. With the current SPICA telescope design, the central obstruction is expected to be as large as 20% of the pupil diameter. The lowest IWA, measured along the diagonal in the coronagraphic image, cannot be smaller than about $5\lambda/D$ for a contrast of 10^{-6}–10^{-7}.

Two of these masks (Fig. 4, right panel) have been fabricated by the National Institute of Advanced Industrial Science and Technology using the ion etching process, and then tested at ISAS. The test design was chosen to be of the type 'bar-code' [21], or its 2-D version, the 'checkerboard' mask [24]. The first mask (Mask 1, Fig. 4(a)) has a very large inner working angle ($8\lambda/D$) because it was designed to match the current 30% central obscuration of the SPICA telescope (which included a baffle at the secondary location). In our first attempts, the PSF exhibited a peak-to-valley contrast ratio of about 10^{-5} along the diagonal direction relative to the mask orientation. At first we thought the discrepancy between the theoretical value and the observed contrast was due to the many small manufacturing artifacts of the mask, which was rejected after some numerical simulations were carried out. However, we discovered that one of the limitations was caused by the diffusion and scattering of light within the camera optics. Therefore, we used a near-to-focal plane square diaphragm to prevent the photons of the bright PSF area contaminating the dark areas. In our next attempt, the peak contrast went down to less than 10^{-6}, very close to the mask theoretical performance of 10^{-7}, and with an average overall contrast of 2.7×10^{-7} (Fig. 5, top row). A second mask (Mask 2, Fig. 4(b)) was later fabricated. This mask was designed for a clear aperture without central obstruction, a lower IWA of $3\lambda/D$ and a larger OWA of $30\lambda/D$. Here again, with the help of the focal plane diaphragm, we could reach even better average

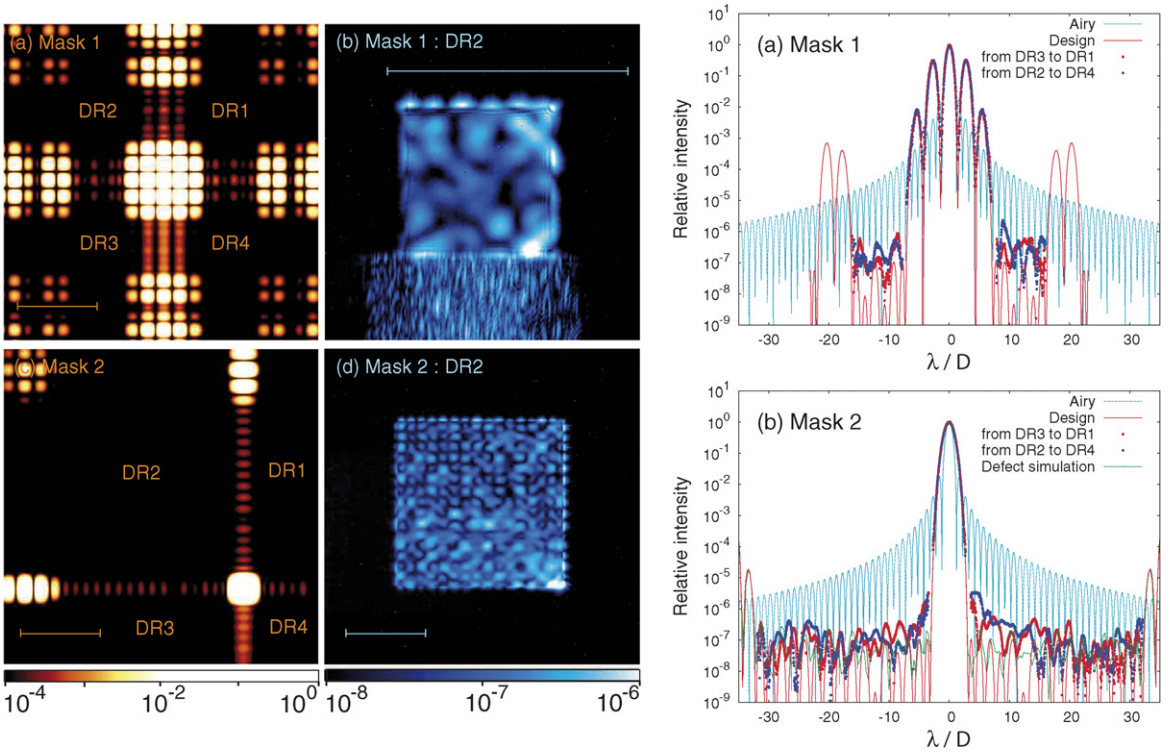

Fig. 5. Laboratory results for the binary checkerboard masks experiment. The left part of the figure shows the recorded image (PSF) for Mask 1 (top) and Mask 2 (bottom), as well as corresponding diagonal cuts profiles (right). The optical axis on the top-left Mask 1 image is centered in the image, whereas it is shifted to the lower right corner of the image for Mask 2 due to the large size of the dark zone.

performance (1.1×10^{-7}, Fig. 5, bottom row) Enya et al. 2007 [25]. Improvements of the optical setup as well as the wavefront compensation by a DM is envisaged as future upgrades. A more detailed study of optimal checkerboard mask design for the SPICA coronagraph is described in Tanaka et al. [26].

4.4. Apodized Lyot and Phase Induced Amplitude Apodized (PIAA) coronagraphs

One of the first concepts proposed for the SPICA coronagraph was the prolate apodized Lyot coronagraph [27]. The formalism of prolate apodized Lyot coronagraphy is extensively described in [27] and [28] and will not be detailed here. These authors show that the correct combination of an apodized pupil with an occulting mask delivers the optimal performance for a Lyot-type coronagraph (i.e. the coronagraphic pupil residual is minimal). As demonstrated by [29], this property is still valid when a central obstruction is present (however, only without spider arms). Other properties make it suitable for cascading occulting masks/Lyot stops in a multi-stage setup, where only one entrance pupil apodizer is used [30]. Each stage provides the same rejection efficiency $\mathbf{Q}$, leading to a final rejection $\mathbf{Q}^N$ if N stages are used. Consequently, if several stages can be used, then some very small occulting masks can be used, as small as $2\lambda/D$ in diameter.

The NAOJ, in collaboration with ISAS, has set up an experiment to validate this concept in the laboratory. Several masks have been designed and manufactured to test several configurations. The masks were manufactured by Canyon Materials Inc. with the HEBS-glass technology [31]. Although some encouraging coronagraphic results were already obtained with HEBS-glass focal plane masks [32], the phase delay introduced by the HEBS-glass [33] turned out to be a very strong limitation to the experiment performance since we did not use adaptive control of the wavefront to compensate for it. These phase aberrations arise from the mask design itself which uses a refractive substrate. A solution to overcome this is to use reflective surfaces in a *two mirror apodization* design, the principle of which is described in, for example, [34] in the context of beam shaping of laser beams. More recently, Guyon [20] and Traub and Vanderbei [35] applied this concept to coronagraphy to produce lossless-flux apodization. As described below, almost arbitrary apodizations can be achieved and thus, extreme contrasts can be obtained in principle.

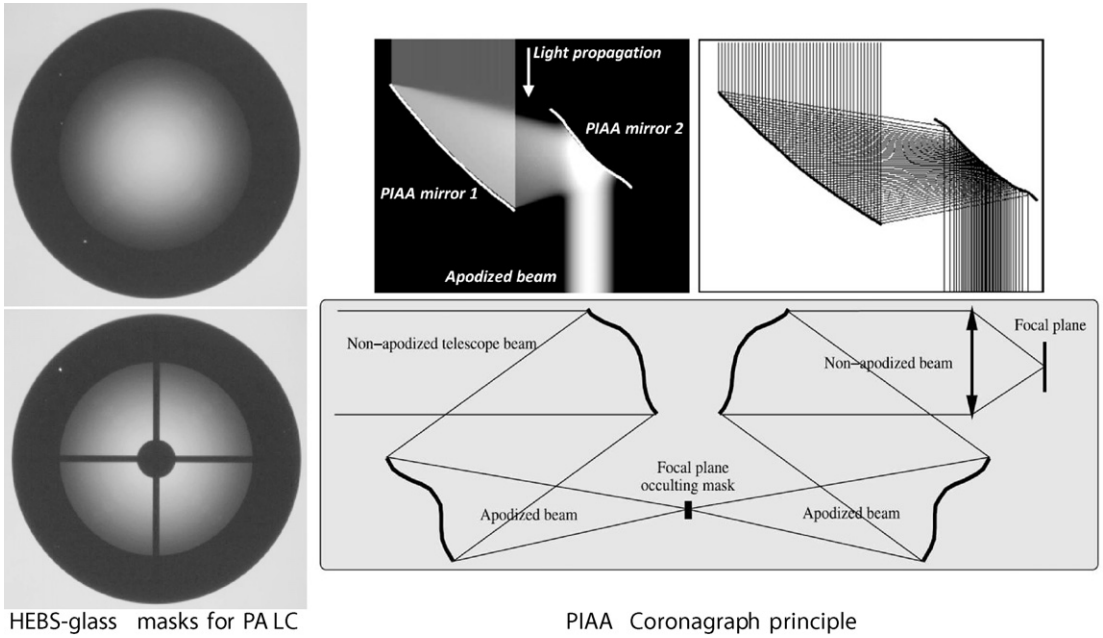

Fig. 6. (Left panel) Two examples of fabricated HEBS-glass masks for the PALC experiment, (top) for a clear aperture, and (bottom) for the SPICA pupil geometry. (Right panel) the PIAA coronagraph principle: (top) the apodization scheme where the light beam is reshaped using aspheric off-axis optics, and (bottom) the implementation of a reversed system, with an intermediate occulting mask to block the central lobe of the PIAA apodized PSF.

As shown on Fig. 6, we can derive the optics shape by using standard ray-tracing methods (by imposing constraints on the conservation of energy and flatness of the wavefront). Another very important property is that the throughput is, in theory, nearly 100%. In practice however, and depending on the tolerances on the optics quality (which should be relaxed in the mid infrared), some additional classical apodizers should be necessary to reach the required contrast, implying some substantial flux losses and a coronagraph throughput probably below 80%. These additional apodizers have three roles: to overcome the natural limitation of PIAA to propagation effects, to mitigate the chromatic propagation effects when working on larger bandwidths, and to relax the optics manufacturing. However, the main drawback is the high distortion of the PSF when the objects are off-axis (off-axis images are basically affected by a strong comatic aberration). This can be overcome by using an inverse set of optics and an intermediate occulting mask to block the light concentrated in the main lobe of the apodized PSF (see Fig. 6).

It is theoretically possible to map a given pupil geometry (with central obstruction and spider arms) to a full, unobscured pupil. However, this has consequences: first, 'filling the geometry gaps' produces a discontinuity wherever some pattern is removed for tilted or more generally perturbed wavefronts. These discontinuities, especially in phase, create some diffraction effects which can degrade the performance. Second, from a manufacturing point of view, removing spider arms requires very aspheric surfaces, with small radius of curvature near the edges. These aspheric surfaces can in practice be manufactured with diamond turning techniques, and additional fine polishing. The most difficult part is the fine polishing step which can be avoided, or at least with less constraints, at longer wavelengths, such as the considered 5–25 μm range. We are currently making an extensive analysis of a PIAA coronagraph for SPICA, including precise wavefront propagation effects, tolerances to manufacturing, and pointing error effects. The PIAA coronagraph, combined with a 32×32 actuators deformable mirror, as well as focal plane wavefront sensing algorithm, are currently being studied by O. Guyon at the Subaru Office (Hilo, Hawaii) in the context of the TPF mission.

5. Conclusion and perspectives

We have described the current status of the SPICA coronagraph project, as well as its role in the more general context of the SPICA mission. We also described the mid to long-term strategy of Japan toward a future terrestrial

planet finder mission, and its efforts in high-contrast imaging instrumentation. It was very good start for us that the coronagraphic performance in our laboratory experiment exceeded the requirement of the SPICA coronagraph using a checkerboard binary shaped pupil mask. Following the success of AKARI, which is an infrared astronomical satellite by ISAS/JAXA, the development of SPICA is ongoing as the next generation infrared mission.

References

[1] M. Mayor, D. Queloz, A Jupiter-mass companion to a solar-type star, Nature 378 (Nov. 23, 1995) 355–359, no. 06555.
[2] G.W. Henry, G.W. Marcy, R.P. Butler, S.S. Vogt, A transiting "51 Peg-like" planet, Astrophys. J. 529 (1) (2000) L41–L44.
[3] D. Charbonneau, T.M. Brown, D.W. Latham, M. Mayor, Detection of planetary transits across a Sun-like star, Astrophys. J. Lett. 529 (2000) 45.
[4] T. Nakagawa, SPICA working group, SPICA: space infrared telescope for cosmology and astrophysics, Adv. Sp. Res. 34 (2004) 645.
[5] T. Onaka, H. Kaneda, K. Enya, T. Nakawaga, H. Murakami, H. Matsuhara, H. Kataza, Development of large aperture cooled telescopes for the Space Infrared Telescope for Cosmology and Astrophysics (SPICA) mission, Proc. SPIE 5494 (2005) 448–462.
[6] M. Tamura, ISAS Report SP 14 (2000) 3.
[7] L. Abe, M. Tamura, T. Nakagawa, K. Enya, S. Tanaka, K. Fujita, J. Nishikawa, N. Murakami, H. Kataza, Current status of the coronagraphic mode for the 3.5 m SPICA space telescope, in: Proc. of the IAU Colloquium 200, 2006, pp. 329–334.
[8] K. Enya, S. Tanaka, T. Nakagawa, H. Kataza, L. Abe, M. Tamura, J. Nishikawa, N. Murakami, K. Fujita, Y. Itoh, Development of an MIR coronagraph for the SPICA mission, Proc. of SPIE 6265 (2006) 626536.
[9] W.A. Traub, et al., TPF-C: status and recent progress, Proc. SPIE 6268 (2006) 62680.
[10] C.A. Beichman, P. Lawson, O. Lay, A. Ahmed, P. Unwin, K. Johnston, Status of the terrestrial planet finder interferometer (TPF-I), Proc. SPIE 6268 (2006) 62680.
[11] A. Léger, J.M. Mariotti, B. Mennesson, M. Ollivier, J.L. Puget, D. Rouan, J. Schneider, The DARWIN Project, Astrophys. Space Sci. 241 (1) (1996) 135–146.
[12] M. Tamura, L. Abe, Direct explorations of exoplanets with the Subaru telescope and beyond, in: Proc. of the IAU Colloquium 200, 2006, pp. 323–328.
[13] K. Murakawa, H. Suto, M. Tamura, N. Kaifu, H. Takami, N. Takato, S. Oya, Y. Hayano, W. Gaessler, Y. Kamata, CIAO: Coronagraphic Imager with Adaptive Optics on the Subaru telescope, Publ. Astron. Soc. Japan 56 (2004) 509–519.
[14] M. Tamura, et al., Concept and science of HiCIAO: high contrast instrument for the Subaru next generation adaptive optics, Proc. SPIE 6269 (2006) 62690.
[15] H. Sugita, T. Nakagawa, H. Murakami, A. Okamoto, H. Nagai, M. Murakami, K. Narasaki, M. Hirabayashi, Cryogenic infrared mission "JAXA/SPICA" with advanced cryocoolers, Cryogenics 46 (2006) 149–157.
[16] R. Hanel, R.B. Conrath, F.M. Flasar, V. Kunde, W. Maquire, J. Pearl, J. Pirraglia, R. Samuelson, L. Horn, P. Schulte, Infrared observations of the Uranian system, Science 233 (1986) 70–74.
[17] B. Conrath, F.M. Flasar, R. Hanel, V. Kunde, W. Maguire, J. Pearl, J. Pirraglia, R. Samuelson, D. Cruikshank, L. Horn, Infrared observations of the Neptunian system, Science 246 (1989) 1454–1459.
[18] T. Guillot, M.S. Marley, D. Saumon, R.S. Freedman, Evolution and Spectra of Extrasolar Giant Planets, Infrared Space Interferometry: Astrophysics & the Study of Earth-Like Planets, Kluwer Academic, 1997, p. 37.
[19] D. Gautier, B. Conrath, M. Flasar, R. Hanel, V. Kunde, A. Chedin, N. Scott, The helium abundance of Jupiter from Voyager, J. Geophys. Res. 86 (Sept. 30, 1981) 8713–8720.
[20] O. Guyon, Phase-induced amplitude apodization of telescope pupils for extrasolar terrestrial planet imaging, Astron. Astrophys. 404 (2004) 379–387.
[21] N.J. Kasdin, R.J. Vanderbei, D.N. Spergel, M.G. Littman, Extrasolar planet finding via optimal apodized-pupil and shaped-Pupil coronagraphs, Astrophys. J. 582 (2003) 1147–1161.
[22] A. Give'On, N.J. Kasdin, R.J. Vanderbei, Y. Avitzour, On representing and correcting wavefront errors in high-contrast imaging systems, J. Opt. Soc. Am. A 23 (5) (2006) 1063–1073.
[23] P. Jacquinot, B. Roizen-Dossier, Progr. Opt. 3 (1964) 29–186.
[24] R.J. Vanderbei, N.J. Kasdin, D.N. Spergel, Checkerboard-mask coronagraphs for high-contrast imaging, Astrophys. J. 615 (2004) 555–561.
[25] K. Enya, S. Tanaka, L. Abe, T. Nakagawa, Laboratory experiment of checkerboard pupil mask coronagraph, Astron. Astrophys. 461 (2007) 783–787.
[26] S. Tanaka, K. Enya, L. Abe, T. Nakagawa, H. Kataza, Binary shaped pupil coronagraphs for high-contrast imaging using a space telescope with central obstructions, Publ. Astron. Soc. Japan 58 (2006) 627–639.
[27] C. Aime, R. Soummer, A. Ferrari, Total coronagraphic extinction of rectangular apertures using linear prolate apodizations, Astron. Astrophys. 389 (2002) 334–344.
[28] R. Soummer, C. Aime, P.E. Falloon, Stellar coronagraphy with prolate apodized circular apertures, Astron. Astrophys. 397 (2003) 1161–1172.
[29] R. Soummer, Apodized pupil Lyot coronagraphs for arbitrary telescope apertures, Astrophys. J. 618 (2005) L161–L164.
[30] C. Aime, R. Soummer, Multiple-stage apodized pupil Lyot coronagraph for high-contrast imaging, Proc. SPIE 5490 (2004) 456–461.
[31] Canyon Materials Inc., http://www.canyonmaterials.com/.
[32] K. Balasubramanian, et al., Occulting focal plane masks for terrestrial planet finder coronagraph: Design, fabrication, simulations and test results, in: C. Aime, F. Vakili (Eds.), Proceedings of the IAU Colloquium, vol. 200, Cambridge University Press, 2006, pp. 405–410.

[33] P. Halverson, M. Ftaclas, K. Balasubramanian, D. Hoppe, D. Wilson, Measurement of wavefront phase delay and optical density in apodized coronagraphic mask materials, Proc. SPIE 5905 (2005) 473–482.
[34] P.H. Malyak, Two mirror unobscured optical system for reshaping the irradiance distribution of a laser beam, Appl. Opt. 31 (22) (1992) 4377–4383.
[35] W.A. Traub, R.J. Vanderbei, Two-mirror apodization for high-contrast imaging, Astrophys. J. 599 (1) (2003) 695–701.